# SUPPORTING INFORMATION

# Highly stable Pd/$HNb_3O_8$-based flexible humidity sensor for perdurable wireless wearable applications

Yuyao Lu[a], Kaichen Xu[a], Min-Quan Yang[b], Shin-Yi Tang[c], Tzu-Yi Yang[c], Yusuke Fujita[a], Satoko Honda[a], Takayuki Arie[a], Seiji Akita[a], Yu-Lun Chueh[c], and Kuniharu Takei*[a,d]

a. *Department of Physics and Electronics, Osaka Prefecture University Sakai, Osaka 599-8531, Japan.*
b. *Fujian Key Laboratory of Pollution Control & Resource Reuse, College of Environmental Science and Engineering, Fujian Normal University Fuzhou, Fujian 350007, China.*
c. *Department of Materials Science and Engineering, National Tsing-Hua University Hsinchu 30013, Taiwan, R.O.C.*
d. *JST PRESTO, Kawaguchi, Saitama 332-0012, Japan.*

*Corresponding author: takei@pe.osakafu-u.ac.jp

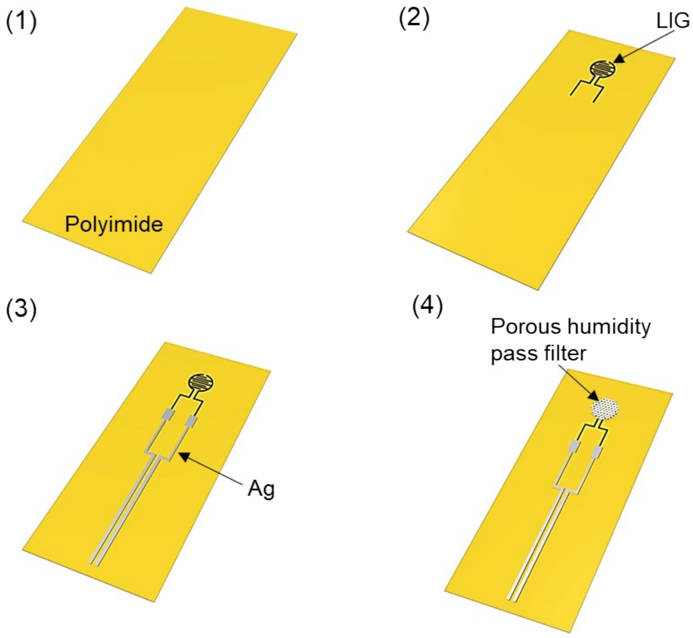


**Figure S1.** Schematics of the fabrication processes for the Pd/$HNb_3O_8$ humidity sensor.

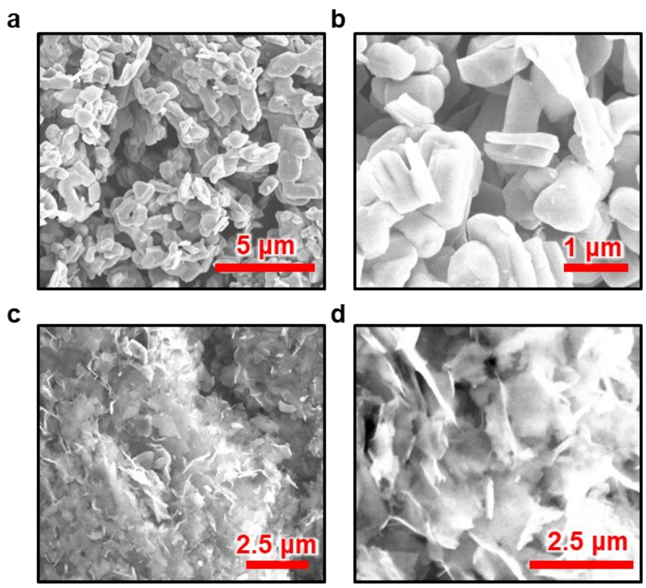


**Figure S2.** SEM images of (a)–(b) bulk $HNb_3O_8$ and (c)–(d) pristine $HNb_3O_8$ nanosheets.

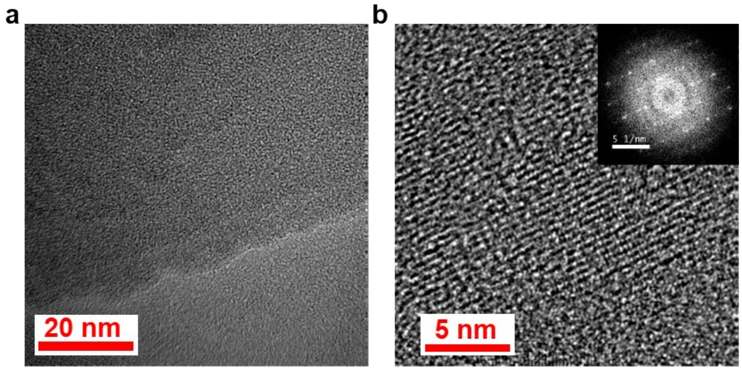


**Figure S3.** (a)(b) TEM images of $HNb_3O_8$ nanosheets.

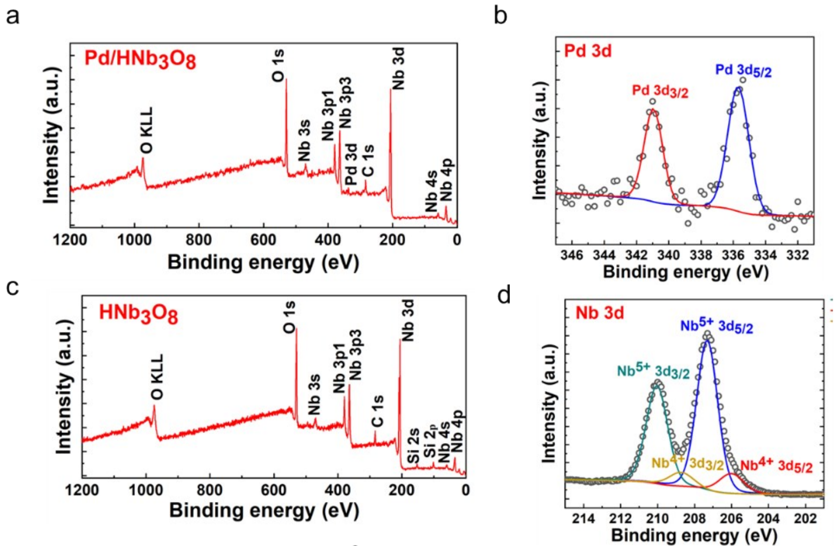


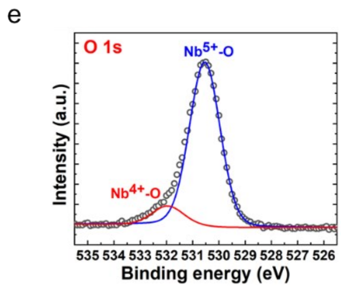


f

| Atomic Ratio | $Nb^{5+}$ | $Nb^{4+}$ | O |
|---|---|---|---|
| $HNb_3O_8$ | 23.34 % | 3.80% | 72.86% |
| $Pd/HNb_3O_8$ | 23.93 % | 4.45% | 71.62% |

**Figure S4.** (a) XPS survey spectrum and (b) Pd 3d spectrum of $Pd/HNb_3O_8$ nanosheets. (c) XPS survey spectrum. (d) Nb 3d and (e) O 1s spectra of pristine $HNb_3O_8$ nanosheets. (f) Table of the atomic ratios of $Nb^{5+}$, $Nb^{4+}$ and O in $HNb_3O_8$ and $Pd/HNb_3O_8$.

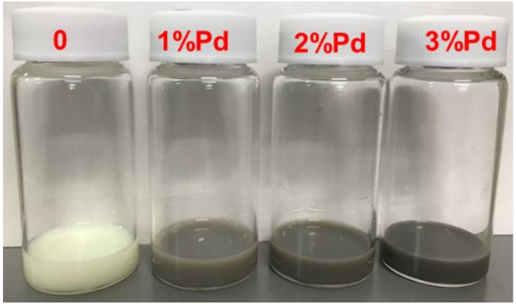


**Figure S5.** Photo of Pd/$HNb_3O_8$ nanosheets solution with different Pd contents.

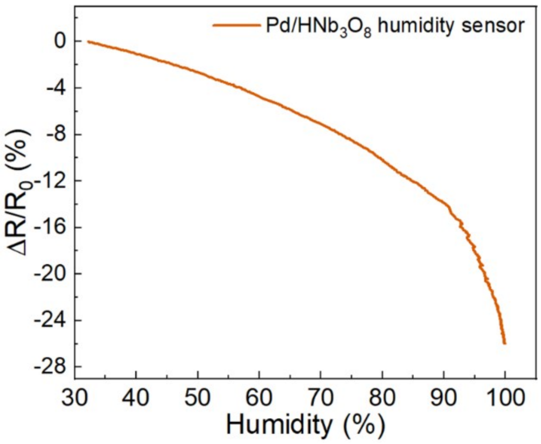


**Figure S6**. Sensitivity test of Pd/$HNb_3O_8$ humidity sensor at humidity variation from 30% to 99.9%.

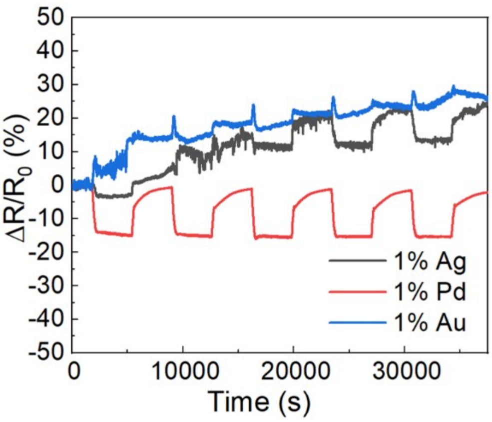


**Figure S7**. Short cycle tests of Ag/Pd/Au-modified $HNb_3O_8$ humidity sensors.

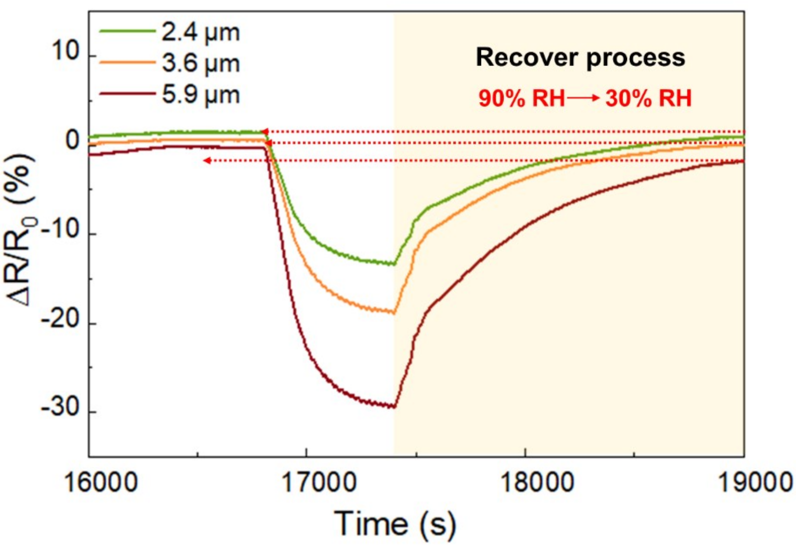


**Figure S8.** The response and recover result of humidity sensors fabricated with different thicknesses of $Pd/HNb_3O_8$ nanosheets.

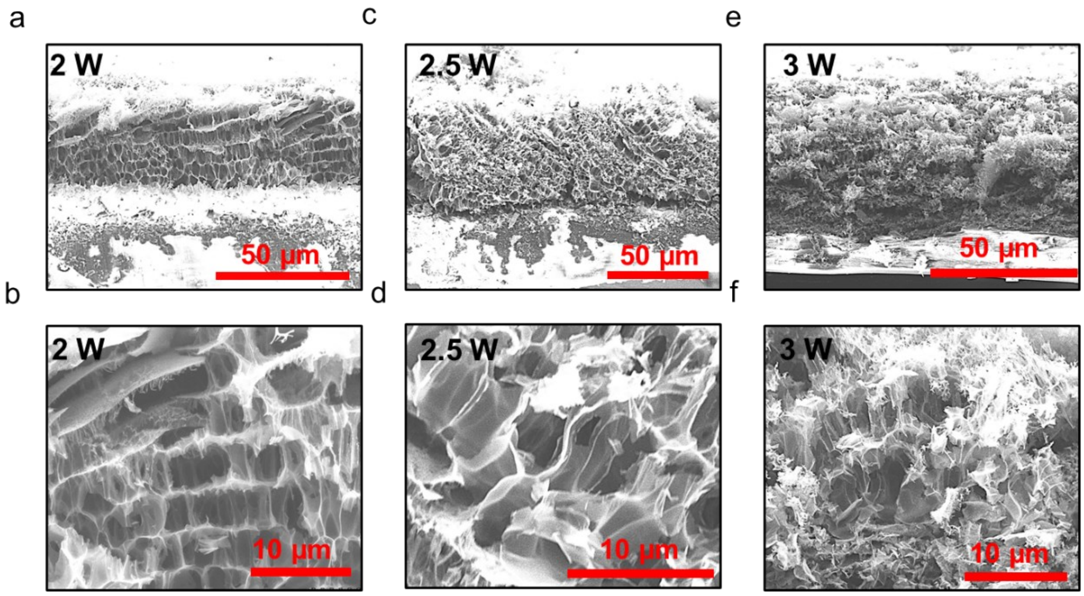


**Figure S9.** Cross-sectional SEM images of LIG generated in different laser powers at (a–b) 2 W, (c–d) 2.5 W, and (e–f) 3 W.

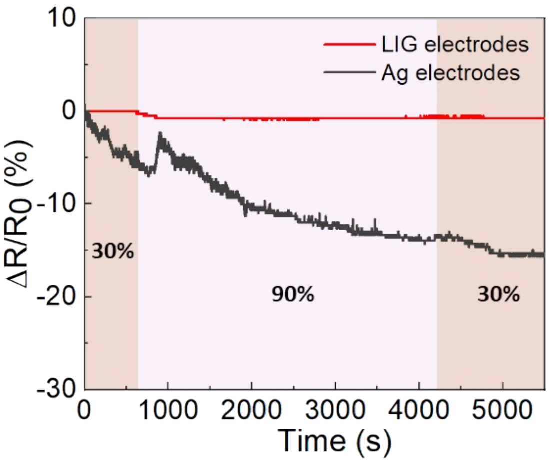


**Figure S10.** Resistance change of LIG electrodes and Ag electrodes under humidity changes from 30% to 90%.

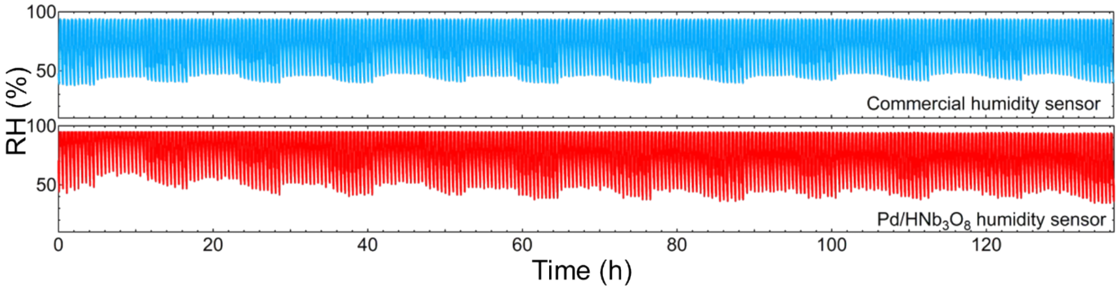


**Figure S11**. 273 cycles of tests at humidity variation from 50% to 90%.

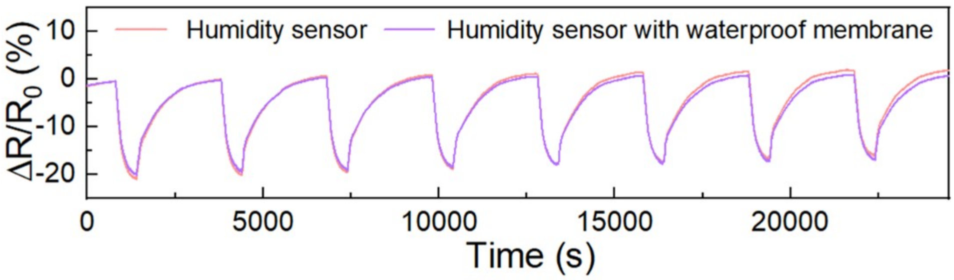


**Figure S12.** Cycle tests of a $Pd/HNb_3O_8$ humidity sensor with and without a porous humidity pass filter.

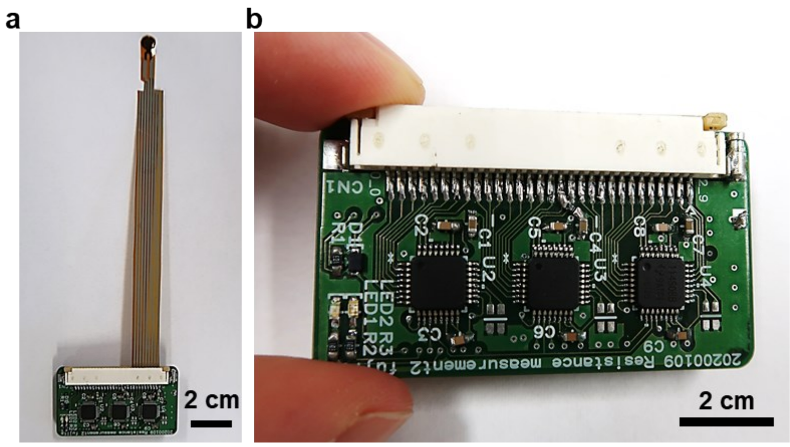


**Figure S13.** (a) Photo of a humidity sensor connected with a microcontroller and wireless circuit. (b) Magnified photo of the circuit.

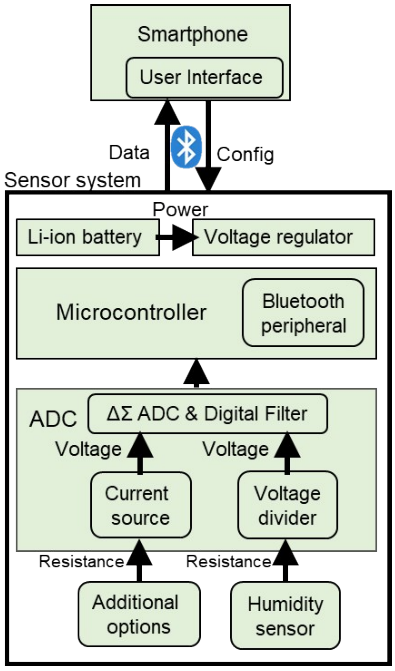


**Figure S14**. Circuit diagram of wireless communication.

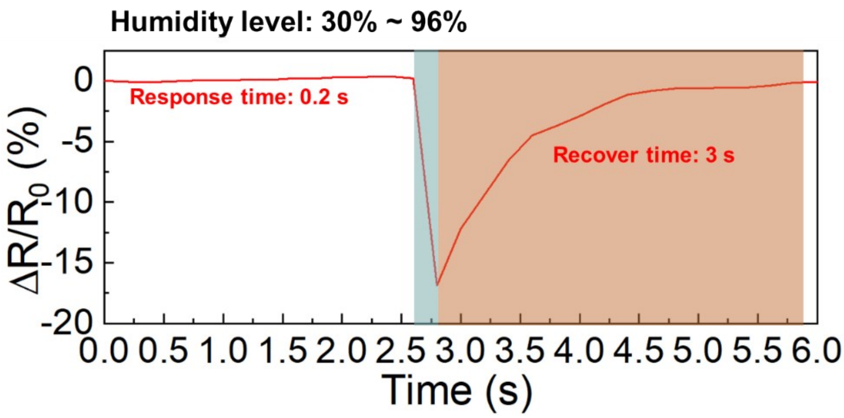


**Figure S15.** Response and recovery times of a short breathing test.

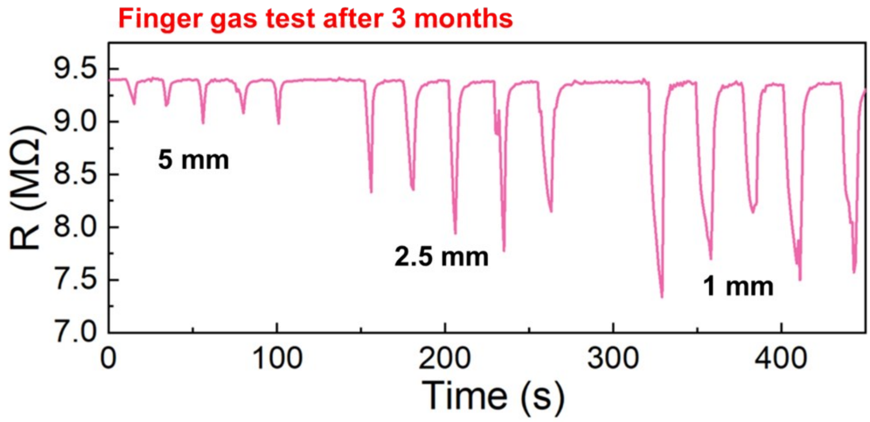


**Figure S16**. The repeated finger moisture detection under different gap distances after 3 months.

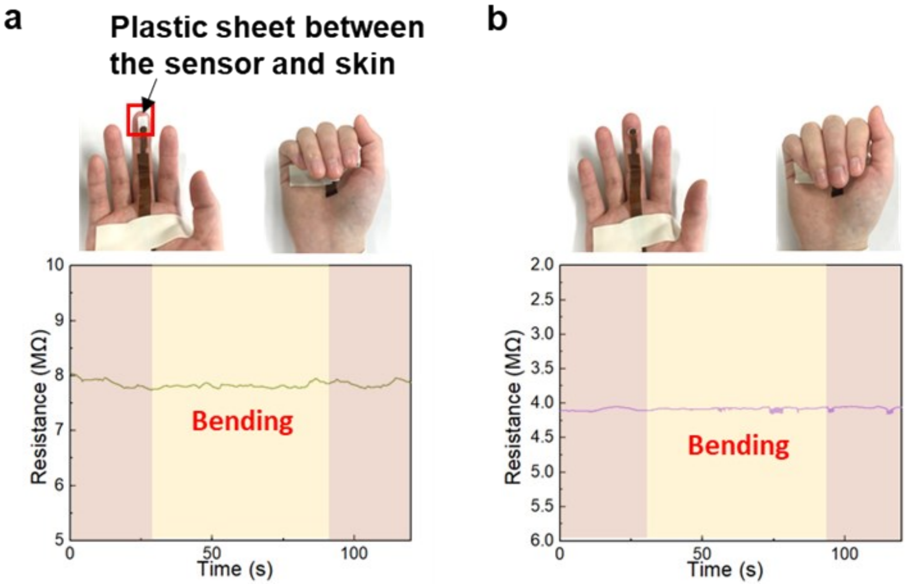


**Figure S17.** Real-time bending result of a humidity sensor placed on the finger of a subject (a) without and (b) with moisture contact.

**Table S1.** Comparison of different material-based humidity sensors.

| Sensing materials | Detection range | Sensitivity at highest RH ($\Delta R/R_0$) | Response /recover time | Cycling number/duration time at high RH | refs |
|---|---|---|---|---|---|
| Pt/nRGO fiber | 6.1%-66.4% | 4.51% | —— | —— | Choi et al. [1] |
| Porous graphene | 12%-97% | 3.21% | 31 s/72 s | 5/5000 s at 59% RH | Pang et al. [2] |
| $MoS_2$ | 0-35% | $10^4$ | 10 s/60 s | 5/500 s at 10% RH | Zhao et al. [3] |
| $VS_2$ nanosheets | 1-100% | —— | 30-40 s/12-50 s | 4/60 s at 60% RH | Feng et al. [4] |
| $WS_2$ | 11%-97% | 469% | 12 s/13 s | 4/250 s at 97.3% RH | Pawbake et al. [5] |
| $MoO_3$ | 0-100% | $10^4$ | 0.5 s/2 s | 5/<15 s at 40% RH | Yang et al. [6] |
| $SnS_2$/RGO | 0-97% | —— | 4 s/3 s for 33% RH, 6 s/15 s for 97% RH | 5/600 s at 97% RH | Zhang et al. [7] |
| P4VP film | 11%-95% | —— | 2.3 s/22.1 s | 7/480 s at 95% RH | Dai et al. [8] |
| Polysaccharide | 11%-95% | 4241.7% | 29 ms/— | 6/200 s at 95% RH | Wang et al. [9] |
| **H-Pd/$HNb_3O_8$ nanosheets** | **30%-99%** | **30%** | **0.2 s/3 s** | **273/137 h at 90% RH** | **This work** |

## References


1. S. J. Choi, H. Yu, J. S. Jang, M. H. Kim, S. J. Kim, H. S. Jeong, I. D. Kim, *Small*, 2018, **14**, 1703934.
2. Y. Pang, J. Jian, T. Tu, Z. Yang, J. Ling, Y. Li, X. Wang, Y. Qiao, H. Tian, Y. Yang, T. L. Ren, *Biosens. Bioelectron.*, 2018, **116**, 123-129.
3. J. Zhao, N. Li, H. Yu, Z. Wei, M. Liao, P. Chen, S. Wang, D. Shi, Q. Sun, G. Zhang, *Adv. Mater.*, 2017, **29**, 1702076.
4. J. Feng, L. Peng, C. Wu, X. Sun, S. Hu, C. Lin, J. Dai, J. Yang, Y. Xie, *Adv. Mater.*, 2012, **24**, 1969-1974.
5. A. S. Pawbake, R. G. Waykar, D. J. Late, S. R. Jadkar, *ACS Appl. Mater. Interfaces*, 2016, **8**, 3359-3365.
6. J. Yang, R. Shi, Z. Lou, R. Chai, K. Jiang, G. Shen, *Small*, 2019, **15**, 1902801.
7. D. Zhang, Z. Xu, Z. Yang and X. Song, *Nano Energy*, 2020, **67**, 104251.
8. J. Dai, H. Zhao, X. Lin, S. Liu, T. Fei and T. Zhang, *Adv. Electron. Mater.*, 2019, **6**, 1900846.
9. L. Wang, Z. Lou, K. Wang, S. Zhao, P. Yu, W. Wei, D. Wang, W. Han, K. Jiang and G. Shen, *Research*, 2020, **2020**, 8716847.